

# Determination of quark–antiquark component of the photon wave function for $u, d, s$ -quarks

A.V. Anisovich, V.V. Anisovich, L.G. Dakhno, V.A. Nikonov,  
A.V. Sarantsev  
( )

Based on the data for the transitions  $\pi^0, \eta, \eta' \rightarrow \gamma\gamma^*(Q^2)$  and reactions of the  $e^+e^-$ -annihilations,  $e^+e^- \rightarrow \rho^0, \omega, \phi$  and  $e^+e^- \rightarrow \text{hadrons}$  at  $1 < E_{e^+e^-} < 3.7$  GeV, we determine the light-quark components of the photon wave function  $\gamma^*(Q^2) \rightarrow q\bar{q}$  ( $q = u, d, s$ ) for the region  $0 \lesssim Q^2 \lesssim 1$  (GeV/c)<sup>2</sup>.

## I. INTRODUCTION

In the search for exotic states one needs to find out the quark–gluon content of mesons and establish meson systematics. The meson radiative decay is a powerful tool for qualitative evaluation of the quark–antiquark components. The study of the two-photon transitions such as  $\text{meson} \rightarrow \gamma\gamma$  and, more generally,  $\text{meson} \rightarrow \gamma^*(Q_1^2)\gamma^*(Q_2^2)$ , looks as a promising way to reveal the quark–antiquark content of mesons.

Experimental data accumulated by the collaborations L3 [1,2], ARGUS [3], CELLO [4], TRC/2 $\gamma$  [5], CLEO [6], Mark II [7], Crystal Ball [8], and others make it obvious that the calculation of the processes  $\text{meson} \rightarrow \gamma^*(Q_1^2)\gamma^*(Q_2^2)$  is up to date. To make this reaction informative as concern the meson quark–gluon content one needs a reliably determined wave function of the photon at  $0 \lesssim Q^2 \lesssim 1$  (GeV/c)<sup>2</sup>. Conventionally, one may consider two pieces of the photon wave function: soft and hard ones. Hard component relates to the point-like vertex  $\gamma \rightarrow q\bar{q}$ , it is responsible for the production of quark–antiquark pair at high virtuality. At large energy of the  $e^+e^-$  system, the ratio of cross sections  $R = \sigma(e^+e^- \rightarrow \text{hadrons})/\sigma(e^+e^- \rightarrow \mu^+\mu^-)$  is determined by the hard component of photon wave function, while soft component is responsible for the production of low-energy quark–antiquark vector states such as  $\rho^0, \omega, \phi(1020)$ , and their excitations.

Evaluation of the photon wave function for the  $\gamma^*(Q^2) \rightarrow u\bar{u}, d\bar{d}, s\bar{s}$  transitions was carried out in [9], on the basis of data of the CLEO Collaboration on the  $Q^2$ -dependent transition form factors  $\pi^0 \rightarrow \gamma\gamma^*(Q^2)$ ,  $\eta \rightarrow \gamma\gamma^*(Q^2)$ , and  $\eta' \rightarrow \gamma\gamma^*(Q^2)$ , see [6] and references therein. The goal of the present paper is, by adding the information on the process  $e^+e^- \rightarrow \text{hadrons}$ , to define more precisely the wave function  $\gamma^*(Q^2) \rightarrow u\bar{u}, d\bar{d}, s\bar{s}$ .

Similarly to what has been done in [9], here we determine photon wave function working in the approach of the spectral integration technique. This technique had been suggested in [10] for the description of deuteron form factors, the deuteron being treated as a composite two-nucleon system. In [9,11], the spectral integration technique was expanded for the composite  $q\bar{q}$  systems with wave functions written in terms of the light-cone variables. The wave function depends on the invariant energy squared of  $q\bar{q}$  system as follows:

$$s = \frac{m^2 + k_{\perp}^2}{x(1-x)}, \quad (1)$$

where  $m$  is the quark mass and  $\mathbf{k}_{\perp}$  and  $x$  are the light cone characteristics of quarks (transverse momentum and a part of longitudinal momentum). In this technique the quark wave function of the photon,  $\gamma^*(Q^2) \rightarrow q\bar{q}$ , is defined as follows:

$$\psi_{\gamma^*(Q^2) \rightarrow q\bar{q}}(s) = \frac{G_{\gamma \rightarrow q\bar{q}}(s)}{s + Q^2}, \quad (2)$$

where  $G_{\gamma \rightarrow q\bar{q}}(s)$  is the vertex for the transition of photon into  $q\bar{q}$  state. Rather schematically the vertex function  $G_{\gamma \rightarrow q\bar{q}}(s)$  may be represented as

$$C e^{-bs} + \theta(s - s_0), \quad (3)$$

where the first term stands for the soft component which is due to the transition of photon to vector  $q\bar{q}$  mesons  $\gamma \rightarrow V \rightarrow q\bar{q}$ , while the second one describes the point-like interaction in the hard domain (here the step-function  $\theta(s - s_0) = 1$  at  $s \geq s_0$  and  $\theta(s - s_0) = 0$  at  $s < s_0$ ). The principal characteristics of the soft component of  $G_{\gamma \rightarrow q\bar{q}}(s)$  is the threshold value of the vertex,  $C \exp(-4m^2b)$ , and the rate of its decrease with energy, that is the slope  $b$ . The

hard component of the vertex is characterised by the magnitude  $s_0$ , which is the quark energy squared when the point-like interaction becomes dominant.

In [9], the photon wave function has been found out assuming the quark relative-momentum dependence is the same for all quark vertices:  $g_{\gamma \rightarrow u\bar{u}}(k^2) = g_{\gamma \rightarrow d\bar{d}}(k^2) = g_{\gamma \rightarrow s\bar{s}}(k^2)$ , where we redenoted  $G_{\gamma \rightarrow q\bar{q}}(s) \rightarrow g_{\gamma \rightarrow q\bar{q}}(k^2)$  with  $k^2 = s/4 - m^2$ . The hypothesis of the vertex universality for  $u$  and  $d$  quarks,

$$G_{\gamma \rightarrow u\bar{u}}(s) = G_{\gamma \rightarrow d\bar{d}}(s) \equiv G_{\gamma}(s) , \quad (4)$$

looks rather trustworthy because of the degeneracy of  $\rho$  and  $\omega$  states, though the similarity in the  $k$ -dependence for the nonstrange and strange quarks may be violated. In addition, using experimental data on the transitions  $\gamma\gamma^*(Q^2) \rightarrow \pi^0, \eta, \eta'$  only one cannot find out the main parameters ( $C, b, s_0$ ) both for  $G_{\gamma \rightarrow s\bar{s}}(s)$  and  $G_{\gamma}(s)$ . In the present paper we add the  $e^+e^-$  annihilation data for the determination of wave functions, that is,  $e^+e^- \rightarrow \gamma^* \rightarrow \rho^0, \omega, \phi(1020)$  together with the ratio  $R(E_{e^+e^-}) = \sigma(e^+e^- \rightarrow \text{hadrons})/\sigma(e^+e^- \rightarrow \mu^+\mu^-)$  at  $E_{e^+e^-}$  higher than 1 GeV. The reactions  $e^+e^- \rightarrow \gamma^* \rightarrow \rho^0, \omega, \phi(1020)$  are rather sensitive to the parameters  $C, b$  of the soft component of photon wave function, while the data on  $R(E_{e^+e^-})$  allow us to fix the parameter  $s_0$  for the beginning of the point-like vertex regime, see Eq. (3).

The paper is organised as follows. In Section 2, which is in fact the introductory one, we present the formulae for the charge form factor of pseudoscalar meson and transition form factors  $\pi^0, \eta, \eta' \rightarrow \gamma(Q_1^2)\gamma(Q_2^2)$  in terms of the spectral integration technique. In Section 3 we consider the  $e^+e^-$  annihilation processes: the partial decay widths  $\omega, \rho^0, \phi \rightarrow e^+e^-$  and the ratio  $R(E_{e^+e^-}) = \sigma(e^+e^- \rightarrow \text{hadrons})/\sigma(e^+e^- \rightarrow \mu^+\mu^-)$  at  $1 \leq E_{e^+e^-} \leq 3.7$  GeV. The photon wave function  $\gamma \rightarrow q\bar{q}$  for the light quarks is determined in Section 4. The results of calculations for the decays  $f_0(980), a_0(980) \rightarrow \gamma\gamma$  and  $f_2(1270), f_2(1525), a_2(1320) \rightarrow \gamma\gamma$  carried out with the found here photon wave function are compared with calculations performed with the old photon wave function [9] in Section 5. In Conclusion, we briefly summarize the results.

## II. QUARK-ANTIQUARK STATE FORM FACTORS IN THE SPECTRAL INTEGRATION TECHNIQUE

In this Section we recall the main formulae for the calculation of the charge and transition form factors in the spectral integration technique, these formulae are used for the determination of photon wave function. First, we present formulae for the charge pion form factor — they are needed to fix up the wave function of the pion and other members of the lowest pseudoscalar nonet,  $\eta$  and  $\eta'$ . The calculation of the charge form factor is based on a principal hypothesis of the additive quark model: the mesons consist of quark and antiquark, and the photon interacts with one of constituent quarks. Hereafter the formulae for the transitions  $\pi^0, \eta, \eta' \rightarrow \gamma(Q_1^2)\gamma(Q_2^2)$  are given, they are written within similar approach. More detailed discussion of these formulae and basic assumptions may be found in [12-21].

### A. Pion charge form factor

Here we recall the logic of calculation in the spectral integration technique and write down the formulae for pion form factor.

General structure of the amplitude of pion-photon interaction is as follows:

$$A_{\mu}^{(\pi)} = e(p_{\mu} + p'_{\mu})F_{\pi}(Q^2) , \quad (5)$$

where  $e$  is the absolute value of electron charge,  $p$  and  $p'$  are pion incoming-outgoing four-momenta, and  $F_{\pi}(Q^2)$  is the pion form factor. We are working in the space-like region of the momentum transfer, so  $Q^2 = -q^2$ , where  $q = p - p'$ . The amplitude  $A_{\mu}^{(\pi)}$  is the transverse one:  $q_{\mu}A_{\mu}^{(\pi)} = 0$ .

In the quark model, the pion form factor is defined as a process shown in Fig. 1a: the photon interacts with one of constituent quarks. In the spectral integration technique, the method of calculation of the diagram of Fig. 1a is as follows: we consider the dispersive integrals over masses of incoming and outgoing  $q\bar{q}$  states, corresponding cuttings of the triangle diagram are shown in Fig. 1b. In this way we calculate the double discontinuity of the triangle diagram,  $\text{disc}_s \text{disc}_{s'} F_{\pi}(s, s', Q^2)$ , where  $s$  and  $s'$  are the energy squares of the  $q\bar{q}$  systems before and after the photon emission,  $P^2 = s$  and  $P'^2 = s'$  (recall, in the dispersion relation technique the momenta of intermediate particles do not coincide with external momenta,  $p \neq P$  and  $p' \neq P'$ ). The double discontinuity is defined by three factors:

(i) product of the pion vertex functions and quark charge:

$$e_q G_\pi(s) G_\pi(s'), \quad (6)$$

where, due to Eq. (5),  $e_q$  is given in the units of the charge  $e$ ,

(ii) phase space of the triangle diagram (Fig. 1b) at  $s \geq 4m^2$  and  $s' \geq 4m^2$ :

$$d\Phi_{\text{tr}} = d\Phi_2(P; k_1, k_2) d\Phi_2(P'; k'_1, k'_2) (2\pi)^3 2k_{20} \delta^{(3)}(\mathbf{k}_2 - \mathbf{k}'_2), \quad (7)$$

with the two-particle phase space determined as:

$$d\Phi_2(P; k_1, k_2) = \frac{1}{2} \frac{d^3 k_1}{(2\pi)^3 2k_{10}} \frac{d^3 k_2}{(2\pi)^3 2k_{20}} (2\pi)^4 \delta^{(4)}(P - k_1 - k_2), \quad (8)$$

(iii) spin factor  $S_\pi(s, s', Q^2)$  determined by the trace of the triangle diagram process of Fig. 1b:

$$-\text{Tr} \left[ i\gamma_5 (m - \hat{k}_2) i\gamma_5 (m + \hat{k}'_1) \gamma_\mu^\perp (m + \hat{k}_1) \right] = (P + P')_\mu^\perp S_\pi(s, s', Q^2). \quad (9)$$

Recall that in the dispersion integral we deal with mass-on-shell particles, so  $k_1^2 = k_1'^2 = k_2^2 = m^2$ . The vertex  $i\gamma_5$  corresponds to the transition  $\pi \rightarrow q\bar{q}$ , the photon is carrying the momentum  $\tilde{q} = P - P'$ , and the photon momentum square is fixed,  $\tilde{q}^2 = q^2 = -Q^2$ . The transversity of the amplitude  $A_\mu^{(\pi)}$  is guaranteed by the use of  $\gamma_\mu^\perp$  in the trace (9):

$$\gamma_\mu^\perp = g_{\mu\nu}^\perp \gamma_\nu, \quad (10)$$

$$g_{\mu\nu}^\perp = g_{\mu\nu} - \frac{(P'_\mu - P_\mu)(P'_\nu - P_\nu)}{q^2},$$

$$(P + P')_\mu^\perp = \left[ P'_\mu + P_\mu - \frac{P'_\mu - P_\mu}{q^2} (s' - s) \right].$$

The spin factor  $S_\pi(s, s', Q^2)$  reads:

$$S_\pi(s, s', Q^2) = 2 \left[ (s + s' + Q^2) \alpha(s, s', Q^2) - Q^2 \right], \quad (11)$$

$$\alpha(s, s', Q^2) = \frac{s + s' + Q^2}{2(s + s') + (s' - s)^2 / Q^2 + Q^2}.$$

As a result, the the double discontinuity of the diagram with a photon emitted by quark is determined as:

$$e_q G_\pi(s) G_\pi(s') S_\pi(s, s', Q^2) d\Phi_{\text{tr}}. \quad (12)$$

Emission of the photon by antiquark gives similar contribution, with a substitution  $e_q \rightarrow e_{\bar{q}}$ : so the total charge factor for the  $\pi^+$  is the unity,  $e_u + e_{\bar{d}} = 1$ . Then the double discontinuity reads:

$$\text{disc}_s \text{disc}_{s'} F_\pi(s, s', Q^2) = G_\pi(s) G_\pi(s') S_\pi(s, s', Q^2) d\Phi_{\text{tr}}. \quad (13)$$

The form factor  $F_\pi(Q^2)$  is defined as a double dispersion integral as follows:

$$F_\pi(Q^2) = \int_{4m^2}^{\infty} \frac{ds ds'}{\pi \pi} \frac{\text{disc}_s \text{disc}_{s'} F_\pi(s, s', Q^2)}{(s' - m_\pi^2)(s - m_\pi^2)}. \quad (14)$$

When the form factor calculations are performed, it is suitable to operate with the wave function of composite system. In case of a pion the wave function is defined as follows:

$$\Psi_\pi(s) = \frac{G_\pi(s)}{s - m_\pi^2}. \quad (15)$$

There are different ways to work with formula (14), in accordance to different goals, where the  $q\bar{q}$  system is involved. Spectral representation of the form factor appears after the integration in (14) over the momenta of constituents by removing  $\delta$ -functions in the phase space  $d\Phi_{\text{tr}}$ . Then

$$F_\pi(Q^2) = \int_{4m^2}^{\infty} \frac{ds ds'}{\pi \pi} \Psi_\pi(s) \Psi_\pi(s') S_\pi(s, s', Q^2) \frac{\theta(s' s Q^2 - m^2 \lambda(s, s', Q^2))}{16 \sqrt{\lambda(s, s', Q^2)}} , \quad (16)$$

$$\lambda(s, s', Q^2) = (s' - s)^2 + 2Q^2(s' + s) + Q^4 .$$

Here the  $\theta$ -function determines the integration region over  $s$  and  $s'$ :  $\theta(X) = 1$  at  $X \geq 0$  and  $\theta(X) = 0$  at  $X < 0$ .

Another way to present form factor is to remove the integration over the energy squares of the quark-antiquark systems,  $s$  and  $s'$ , by using  $\delta$ -functions entering  $d\Phi_{\text{tr}}$ . Then we have the formula for the pion form factor in the light-cone variables:

$$F_\pi(Q^2) = \frac{1}{16\pi^3} \int_0^1 \frac{dx}{x(1-x)^2} \int d^2 k_\perp \Psi_\pi(s) \Psi_\pi(s') S_\pi(s, s', Q^2) , \quad (17)$$

$$s = \frac{m^2 + k_\perp^2}{x(1-x)} , \quad s' = \frac{m^2 + (\mathbf{k}_\perp - x\mathbf{Q})^2}{x(1-x)} ,$$

where  $\mathbf{k}_\perp$  and  $x$  are the light-cone quark characteristics (transverse momentum of the quark and a part of momentum along the  $z$ -axis).

Fitting formulae (16) or (17) to data at  $0 \leq Q^2 \leq 1$  (GeV/c)<sup>2</sup> with two-exponential parametrization of the wave function  $\Psi_\pi$ :

$$\Psi_\pi(s) = c_\pi [\exp(-b_1^\pi s) + \delta_\pi \exp(-b_2^\pi s)] , \quad (18)$$

we obtain the following values of the pion wave function parameters:

$$c_\pi = 209.36 \text{ GeV}^{-2}, \quad \delta_\pi = 0.01381, \quad b_1^\pi = 3.57 \text{ GeV}^{-2} \quad b_2^\pi = 0.4 \text{ GeV}^{-2} . \quad (19)$$

Figure 2 demonstrates the description of the data by formula (16) (or (17)) with the pion wave function given by (18), (19).

The region  $1 \leq Q^2 \leq 2$  (GeV/c)<sup>2</sup> was not used for the determination of parameters of the pion wave function: one may suppose that at  $Q^2 \geq 1$  (GeV/c)<sup>2</sup> the predictions of additive quark model fail. However, one can see that the calculated curve fits reasonably to data in the neighbouring region  $1 \leq Q^2 \leq 2$  (GeV/c)<sup>2</sup> too (dashed curve in Fig. 2).

The constraint  $F_\pi(0) = 1$  serves us as a normalization condition for pion wave function. We have in the low- $Q^2$  region:

$$F_\pi(Q^2) \simeq 1 - \frac{1}{6} R_\pi^2 Q^2 , \quad (20)$$

with  $R_\pi^2 \simeq 10$  (GeV/c)<sup>-2</sup>. The pion radius is just the characteristics, which is used later on for comparative estimates of the wave function parameters for other low-lying  $q\bar{q}$  states.

## B. Transition form factors $\pi^0, \eta, \eta' \rightarrow \gamma^*(Q_1^2) \gamma^*(Q_2^2)$ .

Using the same technique we can write the formulae for transition form factors of pseudoscalar mesons  $\pi^0, \eta, \eta' \rightarrow \gamma^*(Q_1^2) \gamma^*(Q_2^2)$ , the corresponding diagrams are shown in Fig. 3.

For these processes, general structure of the amplitude is as follows:

$$A_{\mu\nu}(Q_1^2, Q_2^2) = e^2 \epsilon_{\mu\nu\alpha\beta} q_\alpha p_\beta F_{(\pi, \eta, \eta') \rightarrow \gamma\gamma}(Q_1^2, Q_2^2) . \quad (21)$$

In the light-cone variables  $(x, \mathbf{k}_\perp)$ , the expression for the transition form factor  $\pi^0 \rightarrow \gamma^*(Q_1^2)\gamma^*(Q_2^2)$  determined by two processes of Fig. 3a and Fig. 3b reads:

$$F_{\pi \rightarrow \gamma\gamma}(Q_1^2, Q_2^2) = \zeta_{\pi \rightarrow \gamma\gamma} \frac{\sqrt{N_c}}{16\pi^3} \int_0^1 \frac{dx}{x(1-x)^2} \int d^2 k_\perp \Psi_\pi(s) \times \quad (22)$$

$$\times \left( S_{\pi \rightarrow \gamma\gamma}(s, s'_1, Q_1^2) \frac{G_\gamma(s'_1)}{s'_1 + Q_2^2} + S_{\pi \rightarrow \gamma\gamma}(s, s'_2, Q_2^2) \frac{G_\gamma(s'_2)}{s'_2 + Q_1^2} \right),$$

where

$$s = \frac{m^2 + k_\perp^2}{x(1-x)}, \quad s'_i = \frac{m^2 + (\mathbf{k}_\perp - x\mathbf{Q}_i)^2}{x(1-x)}, \quad (i = 1, 2). \quad (23)$$

The spin factor for pseudoscalar states depends on the quark mass only:

$$S_{\pi \rightarrow \gamma\gamma}(s, s'_i, Q_i^2) = 4m. \quad (24)$$

The charge factor for the decay  $\pi^0 \rightarrow \gamma\gamma$  is equal to

$$\zeta_{\pi \rightarrow \gamma\gamma} = \frac{e_u^2 - e_d^2}{\sqrt{2}} = \frac{1}{3\sqrt{2}}. \quad (25)$$

In (22) the ratio  $G_\gamma(s_i)/(s_i + Q^2)$  is the photon wave function (remind, we denote  $G_{\gamma \rightarrow u\bar{u}}(s) = G_{\gamma \rightarrow d\bar{d}}(s) \equiv G_\gamma(s)$ ). The factor  $\sqrt{N_c}$  in the right-hand side of (22) appears due to another definition of the colour wave function of the photon as compared to pion's one: without  $1/\sqrt{N_c}$ .

In terms of the spectral integrals over the  $(s, s')$  variables, the transition form factor for  $\pi^0 \rightarrow \gamma^*(Q_1^2)\gamma^*(Q_2^2)$  reads:

$$F_{\pi \rightarrow \gamma\gamma}(Q_1^2, Q_2^2) = \zeta_{\pi \rightarrow \gamma\gamma} \frac{\sqrt{N_c}}{16} \int_{4m^2}^{\infty} \frac{ds ds'}{\pi \pi} \Psi_\pi(s) \times \quad (26)$$

$$\times \left[ \frac{\theta(s'sQ_1^2 - m^2\lambda(s, s', Q_1^2))}{\sqrt{\lambda(s, s', Q_1^2)}} S_\pi(s, s', Q_1^2) \frac{G_\gamma(s')}{s' + Q_2^2} + \right.$$

$$\left. + \frac{\theta(s'sQ_2^2 - m^2\lambda(s, s', Q_2^2))}{\sqrt{\lambda(s, s', Q_2^2)}} S_\pi(s, s', Q_2^2) \frac{G_\gamma(s')}{s' + Q_1^2} \right],$$

where  $\lambda(s, s', Q_i^2)$  is determined in (16).

Similar expressions may be written for the transitions  $\eta, \eta' \rightarrow \gamma^*(Q_1^2)\gamma^*(Q_2^2)$ . One should bear in mind that, because of the presence of two quarkonium components, their flavour wave functions are:  $s\bar{s}$  and  $n\bar{n} = (u\bar{u} + d\bar{d})/\sqrt{2}$ , in the  $\eta, \eta'$ -mesons,

$$\eta = \sin\theta n\bar{n} - \cos\theta s\bar{s}, \quad \eta' = \cos\theta n\bar{n} + \sin\theta s\bar{s},$$

their transition form factors are expressed through mixing angle  $\theta$  as follows:

$$F_{\eta \rightarrow \gamma\gamma}(s) = \sin\theta F_{\eta/\eta'(n\bar{n}) \rightarrow \gamma\gamma}(s) - \cos\theta F_{\eta/\eta'(s\bar{s}) \rightarrow \gamma\gamma}(s), \quad (27)$$

$$F_{\eta' \rightarrow \gamma\gamma}(s) = \cos\theta F_{\eta/\eta'(n\bar{n}) \rightarrow \gamma\gamma}(s) + \sin\theta F_{\eta/\eta'(s\bar{s}) \rightarrow \gamma\gamma}(s).$$

The spin factors for nonstrange components of  $\eta$  and  $\eta'$  are the same as those for the pion,  $S_{\eta/\eta'(n\bar{n}) \rightarrow \gamma\gamma}(s, s', Q^2) = 4m$ , though with another quark mass entering the strange component: and  $S_{\eta/\eta'(s\bar{s}) \rightarrow \gamma\gamma}(s, s', Q^2) = 4m_s$ .

Charge factors for the  $n\bar{n}$  and  $s\bar{s}$  components are equal to

$$\zeta_{\eta/\eta'(n\bar{n}) \rightarrow \gamma\gamma} = \frac{5}{9\sqrt{2}}, \quad \zeta_{\eta/\eta'(s\bar{s}) \rightarrow \gamma\gamma} = \frac{1}{9}. \quad (28)$$

In the calculation of transition form factors of pseudoscalar mesons, the wave function related to nonstrange quarks in  $\eta$  and  $\eta'$  was assumed to be the same as for the pion:

$$\Psi_{\eta/\eta'(n\bar{n})}(s) = \Psi_{\pi}(s) . \quad (28a)$$

As to strange components of the wave functions, we suppose the same shape for  $n\bar{n}$  and  $s\bar{s}$ . For  $\Psi_{\eta/\eta'(s\bar{s})}(s) = \Psi_{\pi}(s)$ , it results in another normalization only as compared to (28a):

$$\Psi_{\eta/\eta'(s\bar{s})}(s) = c_{\eta/\eta'(s\bar{s})} \left[ \exp(-b_1^{\eta/\eta'(s\bar{s})} s) + \delta_{\eta/\eta'(s\bar{s})} \exp(-b_2^{\eta/\eta'(s\bar{s})} s) \right] , \quad (29)$$

$$c_{\eta/\eta'(s\bar{s})} = 528.78 \text{ GeV}^{3/2} , \quad \delta_{\eta/\eta'(s\bar{s})} = \delta_{\pi} , \quad b_1^{\eta/\eta'(s\bar{s})} = b_1^{\pi} , \quad b_2^{\eta/\eta'(s\bar{s})} = b_2^{\pi} .$$

### III. $E^+E^-$ -ANNIHILATION

The  $e^+e^-$ -annihilation processes provide us with additional information on the photon wave function:

(i) Partial width of the transitions  $\omega, \rho^0, \phi \rightarrow e^+e^-$  is defined by the quark loop diagrams, which contain the product  $G_{\gamma}(s)\Psi_V(s)$ , where  $\Psi_V(s)$  is the quark wave function of vector meson ( $V = \omega, \rho^0, \phi$ ). Supposing that radial wave functions of  $\omega, \rho^0, \phi$  coincide with those of the lowest pseudoscalar mesons (this assumption looks verisimilar, for these mesons are members of the same lowest 36-plet), we can obtain information about  $G_{\gamma}(s)$  and  $G_{\gamma(s\bar{s})}(s)$  from the data on the  $\omega, \rho^0, \phi \rightarrow e^+e^-$  decays [22].

(ii) The ratio  $R(s) = \sigma(e^+e^- \rightarrow \text{hadrons})/\sigma(e^+e^- \rightarrow \mu^+\mu^-)$  at high center-of-mass energies but below the open charm production ( $\sqrt{s} \equiv E_{e^+e^-} < 3.7 \text{ GeV}$ ) is determined by hard components of the photon vertices  $G_{\gamma}(s)$  and  $G_{\gamma(s\bar{s})}(s)$  (transitions  $\gamma^* \rightarrow u\bar{u}, d\bar{d}, s\bar{s}$ ), thus giving us a well-known magnitude  $R(s) = 2$  (small deviations from  $R(s) = 2$  comes from corrections related to the gluon emission  $\gamma^* \rightarrow q\bar{q}g$ , see [23] and references therein). Hence the deviation of the ratio from the value  $R(s) = 2$  at decreasing  $E_{e^+e^-}$  provides us with the information about the energies, when the regime changes: hard components in  $G_{\gamma}(s)$  and  $G_{\gamma(s\bar{s})}(s)$  stop working, while soft components start to play their role.

#### A. Partial decay widths $\omega, \rho^0, \phi \rightarrow e^+e^-$

Figure 4 is a diagrammatic representation of the reaction  $V \rightarrow e^+e^-$ : virtual photon produces the  $q\bar{q}$  pair, which turns into vector meson.

Partial width of vector meson is determined as follows:

$$m_V \Gamma_{V \rightarrow e^+e^-} = \pi \alpha^2 A_{e^+e^- \rightarrow V}^2 \frac{1}{m_V^4} \left( \frac{4}{3} m_V^2 + \frac{8}{3} m_e^2 \right) \sqrt{\frac{m_V^2 - 4m_e^2}{m_V^2}} . \quad (30)$$

Here  $m_V$  is the vector meson mass, the factor  $1/m_V^2$  is associated with photon propagator, and  $\alpha = e^2/(4\pi)$ . In (30), the integration over electron-positron phase space results in  $\sqrt{(m_V^2 - 4m_e^2)}/m_V^2/(16\pi)$ , while the averaging over vector meson polarizations and summing over electron-positron spins gives:

$$\frac{1}{3} \text{Tr} \left[ \gamma_{\mu}^{\perp} (\hat{k}_1 + m_e) \gamma_{\mu}^{\perp} (-\hat{k}_2 + m_e) \right] = \frac{4}{3} m_V^2 + \frac{8}{3} m_e^2 . \quad (31)$$

The amplitude  $A_{V \rightarrow e^+e^-}$  is determined through the quark-antiquark loop calculations, within spectral-integration technique. In this way, we get for the decays  $\omega, \rho^0 \rightarrow e^+e^-$ :

$$A_{\omega, \rho^0 \rightarrow e^+e^-} = Z_{\omega, \rho^0} \frac{\sqrt{N_c}}{16\pi} \int_{4m^2}^{\infty} \frac{ds}{\pi} G_{\gamma}(s) \Psi_{\omega, \rho}(s) \sqrt{\frac{s - 4m^2}{s}} \left( \frac{8}{3} m^2 + \frac{4}{3} s \right) , \quad (32)$$

where  $Z_{\omega, \rho^0}$  is the quark charge factor for vector mesons:  $Z_{\omega} = 1/(3\sqrt{2})$  and  $Z_{\rho^0} = 1/\sqrt{2}$ . We have similar expression for the  $\phi(1020) \rightarrow e^+e^-$  amplitude:

$$A_{\phi \rightarrow e^+ e^-} = Z_\phi \frac{\sqrt{N_c}}{16\pi} \int_{4m_s^2}^{\infty} \frac{ds}{\pi} G_{\gamma \rightarrow s\bar{s}}(s) \Psi_\phi(s) \sqrt{\frac{s-4m_s^2}{s}} \left( \frac{8}{3}m_s^2 + \frac{4}{3}s \right), \quad (33)$$

with  $Z_\phi = 1/3$ . The normalization condition for the vector-meson wave function reads:

$$\frac{1}{16\pi} \int_{4m^2}^{\infty} \frac{ds}{\pi} \Psi_V^2(s) \sqrt{\frac{s-4m^2}{s}} \left( \frac{8}{3}m^2 + \frac{4}{3}s \right) = 1. \quad (34)$$

The wave function is parametrized in one-exponential form:

$$\Psi_V(s) = c_V \exp(-b_V s), \quad (35)$$

with

$$b_{\omega,\rho} = 2.2 \text{ GeV}^{-2}, \quad c_{\omega,\rho} = 95.1 \text{ GeV}^{-2} \quad (36)$$

for the non-strange mesons and

$$b_\phi = 2.5 \text{ GeV}^{-2}, \quad c_\phi(s\bar{s}) = 374.8 \text{ GeV}^{-2} \quad (37)$$

for the  $\phi(1020)$ . Within the used parametrization the vector mesons are characterized by the following mean radii squared:  $R_{\omega,\rho}^2 = 10 (\text{GeV}/c)^{-2}$  and  $R_\phi^2 = 11 (\text{GeV}/c)^{-2}$ .

#### B. The ratio $R(s) = \sigma(e^+e^- \rightarrow \text{hadrons})/\sigma(e^+e^- \rightarrow \mu^+\mu^-)$ at energies below the open charm production

At high energies but below the open charm production,  $E_{e^+e^-} = \sqrt{s} < 3.7 \text{ GeV}$ , the ratio  $R(s)$  is determined by the sum of quark charges squared in the transition  $e^+e^- \rightarrow \gamma^* \rightarrow u\bar{u} + d\bar{d} + s\bar{s}$  multiplied by the factor  $N_c = 3$ :

$$R(s) = \frac{\sigma(e^+e^- \rightarrow \text{hadrons})}{\sigma(e^+e^- \rightarrow \mu^+\mu^-)} = N_c(e_u^2 + e_d^2 + e_s^2) = 2. \quad (38)$$

Since the  $G_\gamma(s)$  and  $G_{\gamma(s\bar{s})}(s)$  vertices are normalized as  $G_\gamma(s) = G_{\gamma(s\bar{s})}(s) = 1$  at  $s \rightarrow \infty$ , we can relate at large  $s$   $R(s)$  and

$$R_{\text{vert}}(s) = 3(e_u^2 + e_d^2)G_\gamma^2(s) + 3e_s^2G_{\gamma(s\bar{s})}^2(s) = \frac{5}{3}G_\gamma^2(s) + \frac{1}{3}G_{\gamma(s\bar{s})}^2(s) \quad (39)$$

to each other:

$$R(s) \simeq R_{\text{vert}}(s). \quad (40)$$

Following (40), we determine the energy region, where the hard components in  $G_\gamma(s)$ ,  $G_{\gamma(s\bar{s})}(s)$  start to dominate.

#### IV. PHOTON WAVE FUNCTION

To determine the photon wave function we use: (i) transition widths  $\pi^0, \eta, \eta' \rightarrow \gamma\gamma^*(Q^2)$ , (ii) partial decay widths  $\omega, \rho^0, \phi \rightarrow e^+e^-, \mu^+\mu^-$ , (iii) the ratio  $R(s) = \sigma(e^+e^- \rightarrow \text{hadrons})/\sigma(e^+e^- \rightarrow \mu^+\mu^-)$ .

Transition vertices for  $u\bar{u}, d\bar{d} \rightarrow \gamma$  and  $s\bar{s} \rightarrow \gamma$  have been chosen in the following form:

$$\begin{aligned} u\bar{u}, d\bar{d}: \quad G_\gamma(s) &= c_\gamma \left( e^{-b_1^\gamma s} + c_2^\gamma e^{-b_2^\gamma s} \right) + \frac{1}{1 + e^{-b_0^\gamma(s-s_0^\gamma)}}, \\ s\bar{s}: \quad G_{\gamma(s\bar{s})}(s) &= c_{\gamma(s\bar{s})} e^{-b_1^{\gamma(s\bar{s})} s} + \frac{1}{1 + e^{-b_0^{\gamma(s\bar{s})}(s-s_0^{\gamma(s\bar{s})})}}. \end{aligned} \quad (41)$$

Recall that photon wave function is determined as  $\Psi_\gamma(s, Q^2) = G_\gamma(s)/(s + Q^2)$ , see Eq. (2).

The following parameter values have been found in fitting to data:

$$\begin{aligned}
u\bar{u}, d\bar{d} : c^\gamma &= 32.577, c_2^\gamma = -0.0187, b_1^\gamma = 4 \text{ GeV}^{-2}, b_2^\gamma = 0.8 \text{ GeV}^{-2}, \\
b_0^\gamma &= 15 \text{ GeV}^{-2}, s_0^\gamma = 1.62 \text{ GeV}^2, \\
s\bar{s} : c_{\gamma(ss)} &= 310.55, b_1^{\gamma(ss)} = 4 \text{ GeV}^{-2}, b_0^{\gamma(ss)} = 15 \text{ GeV}^{-2}, s_0^{\gamma(ss)} = 2.15 \text{ GeV}^2.
\end{aligned} \tag{42}$$

Now let us present the results of the fit in a more detail.

Figure 5 shows the data for  $\pi^0 \rightarrow \gamma\gamma^*(Q^2)$  [4,22],  $\eta \rightarrow \gamma\gamma^*(Q^2)$  [4-6,22] and  $\eta' \rightarrow \gamma\gamma^*(Q^2)$  [2,4-6,22]. We perform the fitting procedure in the interval  $0 \leq Q^2 \leq 1$  (GeV/c)<sup>2</sup>, the fitting curves are shown by solid lines. The continuation of the curves into neighbouring region  $1 \leq Q^2 \leq 2$  (GeV/c)<sup>2</sup> (dashed lines) demonstrates that there is also reasonable description of the data.

The calculation results for the  $V \rightarrow e^+e^-$  decay partial widths *versus* data [22] are shown below (in keV):

$$\begin{aligned}
\Gamma_{\rho^0 \rightarrow e^+e^-}^{\text{calc}} &= 7.50, & \Gamma_{\rho^0 \rightarrow e^+e^-}^{\text{exp}} &= 6.77 \pm 0.32, \\
\Gamma_{\omega \rightarrow e^+e^-}^{\text{calc}} &= 0.796, & \Gamma_{\omega \rightarrow e^+e^-}^{\text{exp}} &= 0.60 \pm 0.02, \\
\Gamma_{\phi \rightarrow e^+e^-}^{\text{calc}} &= 1.33, & \Gamma_{\phi \rightarrow e^+e^-}^{\text{exp}} &= 1.32 \pm 0.06, \\
\Gamma_{\rho^0 \rightarrow \mu^+\mu^-}^{\text{calc}} &= 7.48, & \Gamma_{\rho^0 \rightarrow \mu^+\mu^-}^{\text{exp}} &= 6.91 \pm 0.42, \\
\Gamma_{\phi \rightarrow \mu^+\mu^-}^{\text{calc}} &= 1.33, & \Gamma_{\phi \rightarrow \mu^+\mu^-}^{\text{exp}} &= 1.65 \pm 0.22.
\end{aligned} \tag{43}$$

Figure 6a demonstrates the data for  $R(s)$  [23] at  $E_{e^+e^-} > 1$  GeV (dashed area) versus  $R_{\text{vert}}(s)$  given by Eq. (39) with parameters (42) (solid line).

In Fig. 6b,c one can see the  $k^2$ -dependence of photon wave functions on the quark relative momentum square  $k^2$  (here  $s = 4m^2 + 4k^2$ ) for the nonstrange and strange components found in our fit (solid line) and that found in [9] (dashed lines). One may see that in the region  $0 \leq k^2 \leq 2.0$  (GeV/c)<sup>2</sup> the scrupulous distinction is rather considerable, though in the average the old and new wave functions almost coincide. In the next section we compare the results obtained for the two-photon decays of scalar and tensor mesons,  $S \rightarrow \gamma\gamma$  and  $T \rightarrow \gamma\gamma$  calculated with old and new wave functions.

## V. TRANSITIONS $S \rightarrow \gamma\gamma$ AND $T \rightarrow \gamma\gamma$

As was mentioned above, in the average the old [9] and new photon wave functions coincide, though they differ in details. So it would be useful to understand to what extent this difference influences the calculation results for the two-photon decays of scalar and tensor mesons.

The calculation of the two-photon decays of scalar mesons  $f_0(980) \rightarrow \gamma\gamma$  and  $a_0(980) \rightarrow \gamma\gamma$  have been performed in [12,13] with old wave function, under the assumption that  $f_0(980)$  and  $a_0(980)$  are the  $q\bar{q}$  systems. The results of the calculations are shown in Fig. 7 (dashed line). Solid curve shows the values found with new photon wave function; for  $a_0(980)$ , new wave function reveals stronger dependence on the radius squared as compared to the old wave function. In the region  $R_{a_0(980)}^2 \sim R_\pi^2 = 10$  (GeV/c)<sup>-2</sup>, the value  $\Gamma(a_0(980) \rightarrow \gamma\gamma)$  calculated with new wave function becomes 1.5–2 times smaller as compared to old wave function — this reflects more precise definition of photon wave function. In the calculations, the flavour wave function of  $f_0(980)$  was defined as follows:

$$f_0(980) : \quad n\bar{n} \cos \varphi + s\bar{s} \sin \varphi.$$

In Fig. 8, the calculated areas are shown for the region  $\varphi < 0$  that is governed by the  $K$ -matrix analysis results of meson spectra [24,25]. Shaded area responds to the experimental data [26].

The  $f_0(980)$  being the  $q\bar{q}$  system is characterized by two parameters: the mean radius squared of  $f_0(980)$  and mixing angle  $\varphi$ . In Fig. 9 the areas allowed for these parameters are shown; they were obtained for the processes  $f_0(980) \rightarrow \gamma\gamma$  and  $\phi(1020) \rightarrow \gamma f_0(980)$  with old photon wave function (Fig. 9a) and new one (Fig. 9b). The change of the allowed areas ( $R_{f_0(980)}^2, \varphi$ ) for the reaction  $f_0(980) \rightarrow \gamma\gamma$  is rather noticeable, but it should be emphasized that it does not lead to a cardinal alteration of the parameter magnitudes.

Another set of reactions calculated with photon wave function is the two-photon decay of tensor mesons as follows  $a_2(1320) \rightarrow \gamma\gamma$ ,  $f_2(1270) \rightarrow \gamma\gamma$  and  $f_2(1525) \rightarrow \gamma\gamma$ . The calculations of  $a_2(1320) \rightarrow \gamma\gamma$  with old and new wave functions are shown in Fig. 10 (dotted and solid lines, respectfully), experimental data [22,26] are presented in Fig. 10 too (shaded areas). The description of experimental data has been carried out at  $R_{a_2(1320)}^2 \sim 8$  (GeV/c)<sup>-2</sup>: in this region the difference between the calculated values of partial widths, which is due to a change of wave function, is of the order of 10–20%.

The amplitude of the transition  $f_2 \rightarrow \gamma\gamma$  is determined by four form factors related to existence of two flavour components and two spin structures, see [12,14] for the details. The calculations of these four form factors with old and new wave functions are shown in Fig. 11 — at  $R_T^2 \sim 8-10$  (GeV/c) $^{-2}$  the difference is of the order of 10–20%. In Fig. 12, we show the allowed areas  $(R_T^2, \varphi_T)$  obtained in the description of experimental widths  $\Gamma(f_2(1270) \rightarrow \gamma\gamma)$  and  $\Gamma(f_2(1525) \rightarrow \gamma\gamma)$  [22] with old (Fig. 12a) and new (Fig. 12b) wave functions. The new photon wave function results in a more rigid constraint for the areas  $(R_T^2, \varphi_T)$ , though there is no qualitative changes in the description of data. The two-photon decay data give us two solutions for the  $(R_T^2, \varphi_T)$ -parameters:

$$\begin{aligned} (R_T^2, \varphi_T)_I &\simeq (8 \text{ (GeV/c)}^{-2}, 0) , \\ (R_T^2, \varphi_T)_{II} &\simeq (8 \text{ (GeV/c)}^{-2}, 25^\circ) . \end{aligned} \tag{44}$$

The solution with  $\varphi \simeq 0$ , when  $f_2(1270)$  is nearly pure  $n\bar{n}$  state and  $f_2(1525)$  is an  $s\bar{s}$  system, is more preferable from the point of view of hadronic decays as well as the analysis [27].

## VI. CONCLUSION

Meson–photon transition form factors have been discussed within various approaches such as perturbative QCD formalism [28,?], QCD sum rules [30-32], variants of the light-cone quark model [9,33-37]. A distinctive feature of the quark model approach [9] consists in taking account of soft interaction of quarks in the subprocess  $\gamma \rightarrow q\bar{q}$ , that is, the account for the production of vector mesons in the intermediate state:  $\gamma \rightarrow V \rightarrow q\bar{q}$ .

In the present paper we have re-analysed the quark components of the photon wave function (the  $\gamma^*(Q^2) \rightarrow u\bar{u}, d\bar{d}, s\bar{s}$  transitions) on the basis of data on the reactions  $\pi^0, \eta, \eta' \rightarrow \gamma\gamma^*(Q^2)$ ,  $e^+e^- \rightarrow \rho^0, \omega, \phi$  and  $e^+e^- \rightarrow \text{hadrons}$ . On the qualitative level, the wave function obtained here coincide with that defined before [9] by using the transitions  $\pi^0, \eta, \eta' \rightarrow \gamma\gamma^*(Q^2)$  only. The data on the reactions  $e^+e^- \rightarrow \rho^0, \omega, \phi$  and  $e^+e^- \rightarrow \text{hadrons}$  allowed us to get the wave function structure more precise, in particular, in the region of the relative quark momenta  $k \sim 0.4 - 1.0$  GeV/c.

Such an improvement of our knowledge of the photon wave function does not lead to a cardinal change in the description of two-photon decays, basis scalar and tensor mesons obtained before [12-14]. Still, a more detailed definition of photon wave function is important for the calculations of the decays of a loosely bound  $q\bar{q}$  state such as radial excitation state or reactions with virtual photons,  $q\bar{q} \rightarrow \gamma^*(Q_1^2)\gamma^*(Q_2^2)$ .

We thank M.G. Ryskin for useful discussions.

This work was supported by the Russian Foundation for Basic Research, project no. 04-02-17091.

- 
- [1] M.N. Kinzle-Focacci, in *Proceedings of the VIIIth Blois Workshop, Protvino, Russia, 28 Jun.–2 Jul. 1999*, ed. by V.A. Petrov and A.V. Prokudin (World Scientific, 2000);  
V.A. Schegelsky, Talk given at Open Session of HEP Division of PNPI *On the Eve of the XXI Century*, 25–29 Dec. 2000.
- [2] M. Acciarri *et al.* (L3 Collab.), *Phys. Lett. B* **501**, 1 (2001); **418**, 389 (1998);  
L. Vodopyanov (L3 Collab.), *Nucl. Phys. Proc. Suppl.* **82**, 327 (2000).
- [3] H. Albrecht *et al.*, (ARGUS Collab.), *Z. Phys. C* **74**, 469 (1997); **65**, 619 (1995); *Phys. Lett. B* **367**, 451 (1994); **267**, 535 (1991).
- [4] H.J. Behrend *et al.* (CELLO Collab.), *Z. Phys. C* **49**, 401 (1991).
- [5] H. Aihara *et al.* (TRC/2 $\gamma$  Collab.), *Phys. Rev. D* **38**, 1 (1988).
- [6] R. Briere *et al.* (CLEO Collab.), *Phys. Rev. Lett.* **84**, 26 (2000).
- [7] F. Butler *et al.* (Mark II Collab.), *Phys. Rev. D* **42**, 1368 (1990).
- [8] K. Karch *et al.* (Crystal Ball Collab.), *Z. Phys. C* **54**, 33 (1992).
- [9] V.V. Anisovich, D.I. Melikhov, and V.A. Nikonov, *Phys. Rev. D* **55**, 2918 (1997).
- [10] V.V. Anisovich, M.N. Kobrinsky, D.I. Melikhov, and A.V. Sarantsev, *Nucl. Phys. A* **544**, 747 (1992);  
A.V. Anisovich and V.A. Sadovnikova, *Yad. Fiz.* **55**, 2657 (1992); **57**, 75 (1994); *Eur. Phys. J. A* **2**, 199 (1998).
- [11] V.V. Anisovich, D.I. Melikhov, and V.A. Nikonov, *Phys. Rev. D* **52**, 5295 (1995).
- [12] A.V. Anisovich, V.V. Anisovich, and V.A. Nikonov, *Eur. Phys. J. A* **12**, 103 (2001).
- [13] A.V. Anisovich, V.V. Anisovich, V.N. Markov, and V.A. Nikonov, *Yad. Fiz.* **65**, 523 (2002) [*Phys. Atom. Nucl.* **65**, 497 (2002)].

- [14] A.V. Anisovich, V.V. Anisovich, M.A. Matveev, and V.A. Nikonov, *Yad. Fiz.* **66**, 946 (2003) [*Phys. Atom. Nucl.* **66**, 914 (2003)].
- [15] A.V. Anisovich, V.V. Anisovich, and V.A. Nikonov, hep-ph/0305216 v2.
- [16] A.V. Anisovich, V.V. Anisovich, V.N. Markov, V.A. Nikonov, A.V. Sarantsev, "*Decay  $\phi(1020) \rightarrow \gamma f_0(980)$ : analysis in the non-relativistic quark model approach*", to be published in *Yad. Fiz.* N 6 (2005), hep-ph/0403123.
- [17] D.I. Melikhov, *Phys. Rev. D* **56**, 7089 (1997); *Phys. Lett. B* **516**, 61 (2001); M. Beyer, D.I. Melikhov, N. Nikitin, and B. Stech, *Phys. Rev. D* **64**:094006 (2001).
- [18] V.V. Anisovich, L.G. Dakhno, V.A. Nikonov, *Yad. Fiz.* **67**, 1593 (2004).
- [19] A.V. Anisovich, V.V. Anisovich, V.N. Markov, M.A. Matveev, and A.V. Sarantsev, *J. Phys. G* **28**, 15 (2002).
- [20] V.V. Anisovich, M.A. Matveev, *Yad. Fiz.* **67**, 634 (2004) [*Phys. Atom. Nucl.* **67**, 614 (2004)].
- [21] A.V. Anisovich, V.V. Anisovich, L. Montanet, and V.A. Nikonov, *Eur. Phys. J. A* **6**, 247 (1999).
- [22] K. Hagiwara *et al.* (Particle Data Group), *Phys. Rev. D* **66**, 1 (2002).
- [23] M.G. Ryskin, A. Martin, and J. Outhwaite, *Phys. Lett. B* **492**, 67 (2000).
- [24] V.V. Anisovich and A.V. Sarantsev, *Eur. Phys. J. A* **16**, 229 (2003).
- [25] V.V. Anisovich, *UFN* **174**, 49 (2004) [*Physics-Uspekhi* **47**, 45 (2004)].
- [26] M. Boggioni and M. Pennington, *Eur. Phys. J. C* **9**, 11 (1999).
- [27] V.A. Schegelsky, *et al.*, hep-ph/0404226.
- [28] G.P. Lepage and S.J. Brodsky, *Phys. Rev. D* **22**, 2157 (1980).
- [29] F.-G. Cao, T. Huang, B.-Q. Ma, *Phys. Rev. D* **53**, 6582 (1996).
- [30] A.V. Radiushkin and R. Ruskov, *Phys. Lett. B* **374**, 173 (1996).
- [31] A. Schmedding and O. Yakovlev, *Phys. Rev. D* **62**, 116002 (2000).
- [32] A.P. Bakulev, S.V. Mikhailov, and N. Stefanis, *Phys. Rev. D* **67**, 074012 (2003).
- [33] C.-W. Hwang, *Eur. Phys. J. C* **19**, 105 (2001).
- [34] H.M. Choi and C.R. Ji, *Nucl. Phys. A* **618**, 291 (1997).
- [35] P. Kroll and M. Raulfus, *Phys. Lett. B* **387**, 848 (1996).
- [36] B.-W. Xiao, B.-Q. Ma, *Phys. Rev. D* **68**, 034020 (2003).
- [37] M.A. DeWitt, H.M. Choi and C.R. Ji, *Phys. Rev. D* **68**, 054026 (2003).

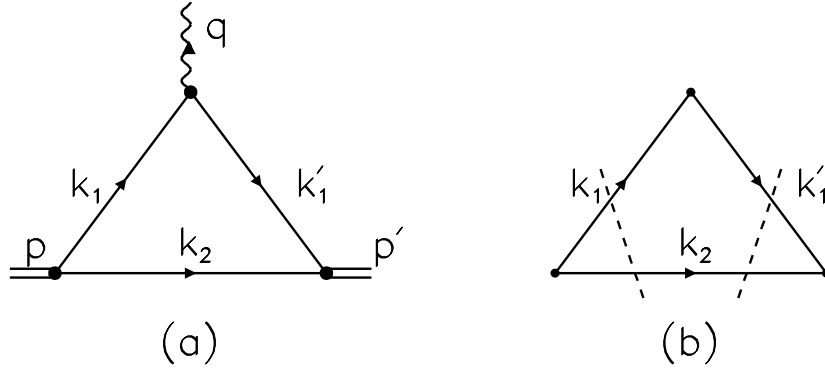


FIG. 1. (a) Diagram for the meson charge form factor in the additive quark model. (b) Cuts of triangle diagram in the spectral integral representation.

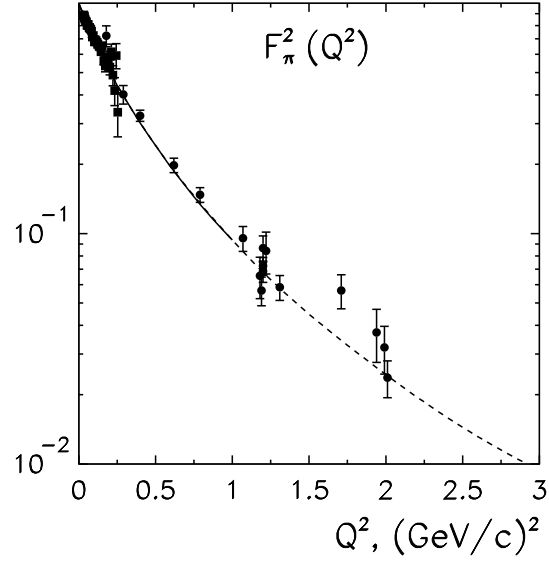


FIG. 2. Description of the experimental data on pion charge form factor with pion wave function given by (18), (19).

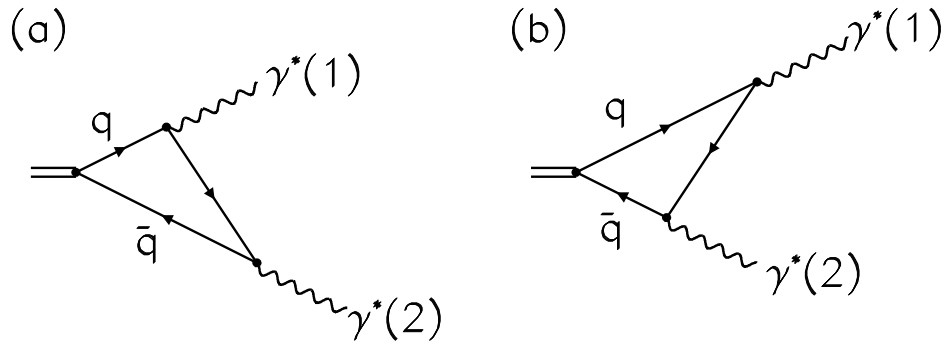


FIG. 3. Diagrams for the two-photon decay of  $q\bar{q}$  state with the emission of photon in the intermediate state by quark (a) and antiquark (b).

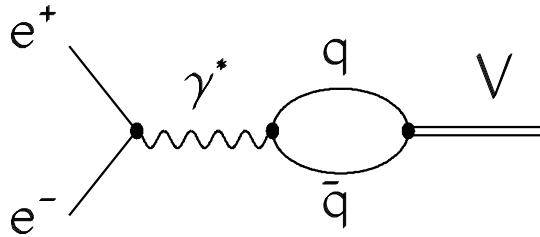


FIG. 4. Production of vector  $q\bar{q}$  state in the  $e^+e^-$ -annihilation.  $V$  denotes the vector meson.

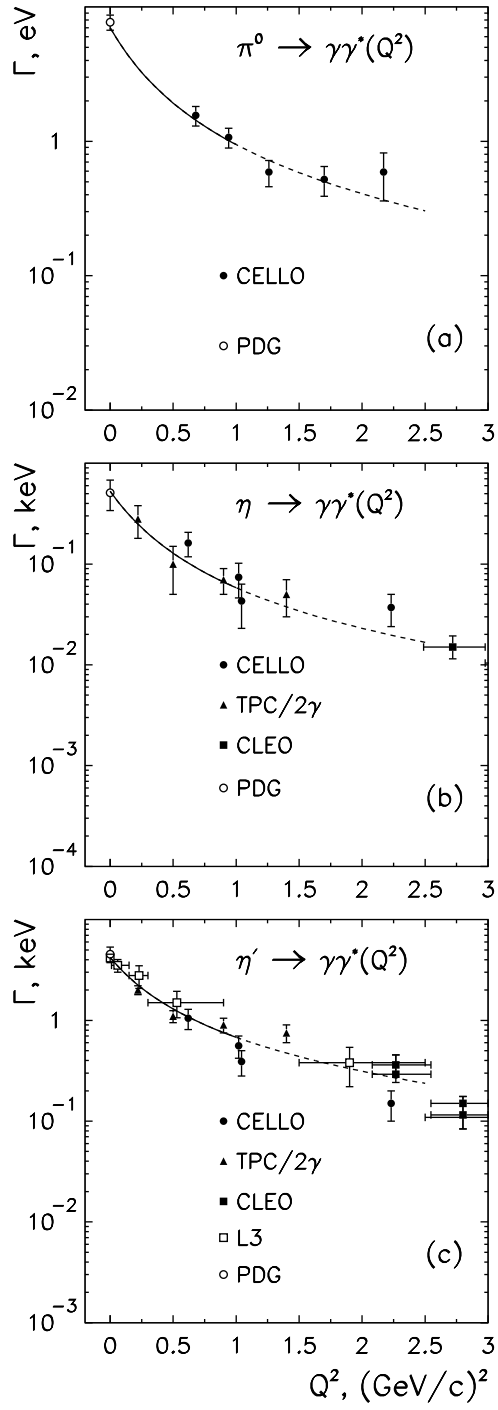


FIG. 5. Data for  $\pi^0 \rightarrow \gamma\gamma^*$ ,  $\eta \rightarrow \gamma\gamma^*$  and  $\eta' \rightarrow \gamma\gamma^*$  vs the calculation curves.

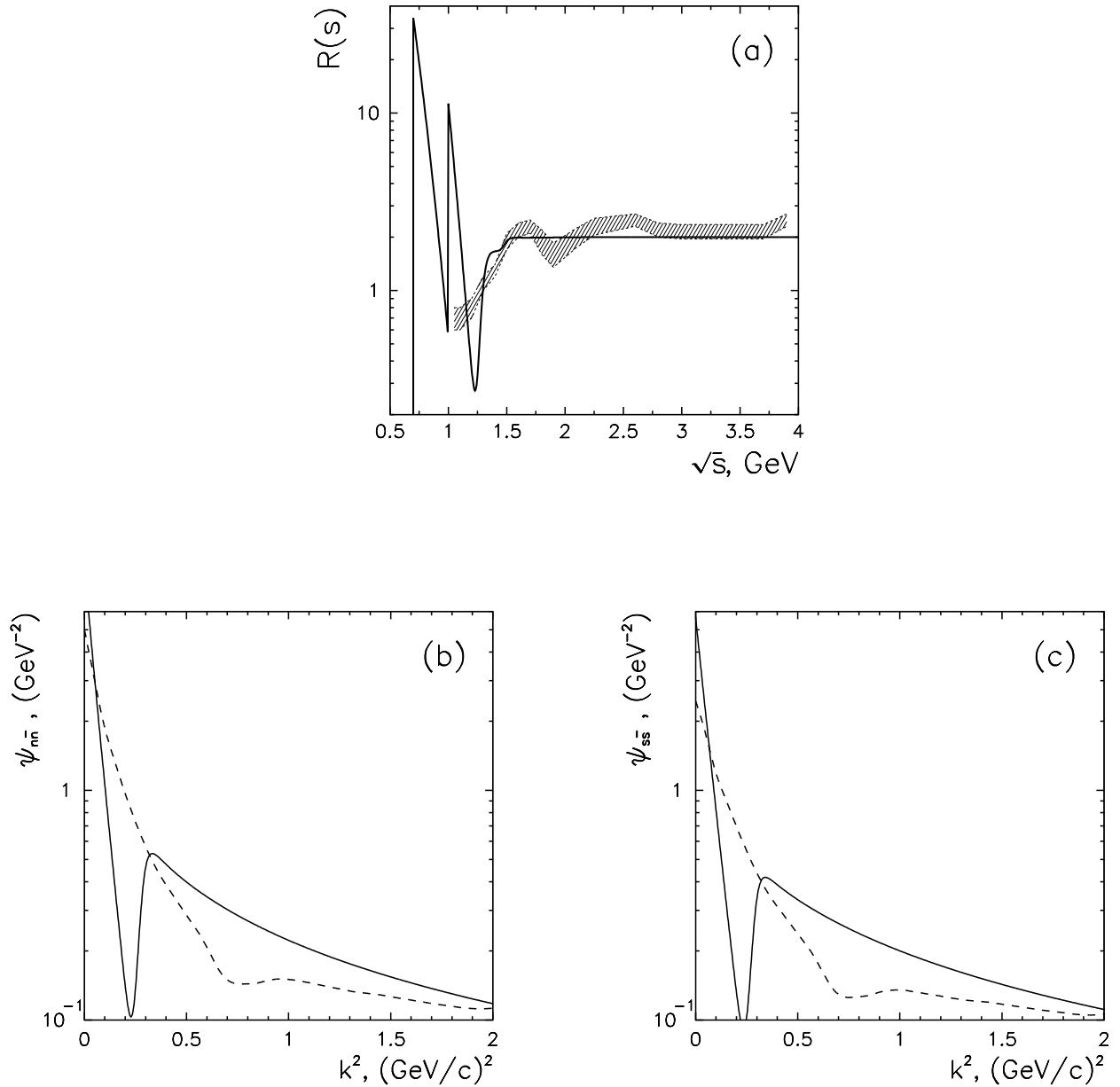


FIG. 6. a)  $R_{\text{vert}}(s)$  (solid line, Eq. (40)) vs  $R(s) = \sigma(e^+e^- \rightarrow \text{hadrons})/\sigma(\mu^+\mu^- \rightarrow \text{hadrons})$  (hatched area); b,c)  $k^2$ -dependence of photon wave function ( $k^2$  is relative quark momentum squared):  $\Psi_{\gamma \rightarrow n\bar{n}}(k^2)$  (b) and  $\Psi_{\gamma \rightarrow s\bar{s}}(k^2)$  (c). Solid curves stand for new wave functions and dashed lines for old one.

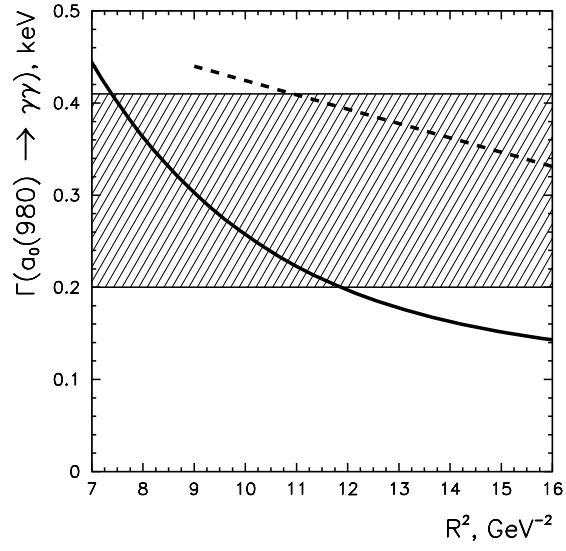


FIG. 7. Partial width  $\Gamma(a_0(980) \rightarrow \gamma\gamma)$  calculated under the assumption that  $a_0(980)$  is  $q\bar{q}$  system, being a function of radius square of  $a_0(980)$ . Solid curve stands for the calculation with new photon wave function, dotted curve stands for old one. Shaded area corresponds to the values allowed by the data [22].

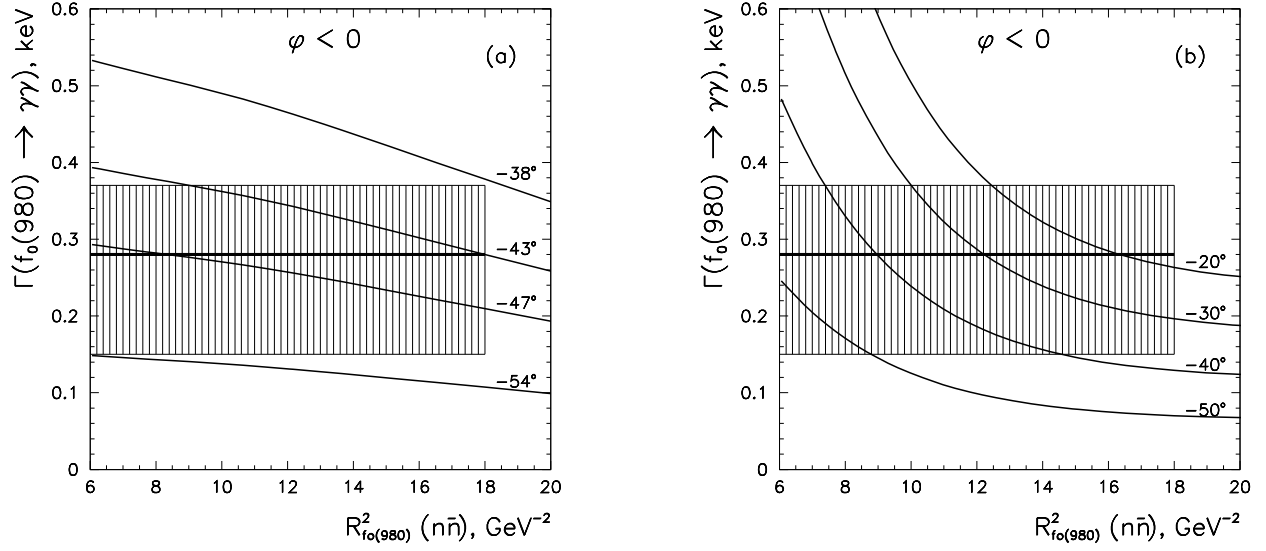


FIG. 8. Partial width  $\Gamma(f_0(980) \rightarrow \gamma\gamma)$  calculated under the assumption that  $f_0(980)$  is  $q\bar{q}$  system,  $q\bar{q} = n\bar{n} \cos \varphi + s\bar{s} \sin \varphi$ , depending on radius squared of the  $q\bar{q}$  system: (a) with old photon wave function, (b) with new one. Calculations were carried out with different values of mixing angle  $\varphi$  in the region  $\varphi < 0$ . Shaded area shows the allowed experimental values [26].

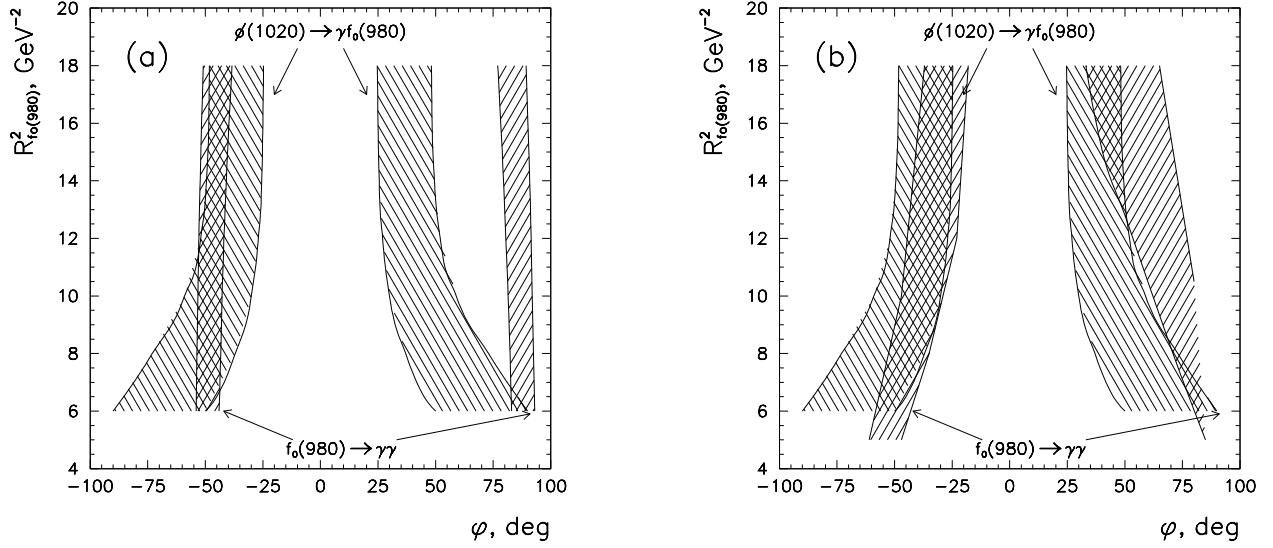


FIG. 9. Combined presentation of the  $(R_{f_0(980)}^2, \varphi)$  areas allowed by the experiment for the decays  $f_0(980) \rightarrow \gamma\gamma$  and  $\phi(1020) \rightarrow \gamma f_0(980)$  with old (a) photon wave function and new one (b).

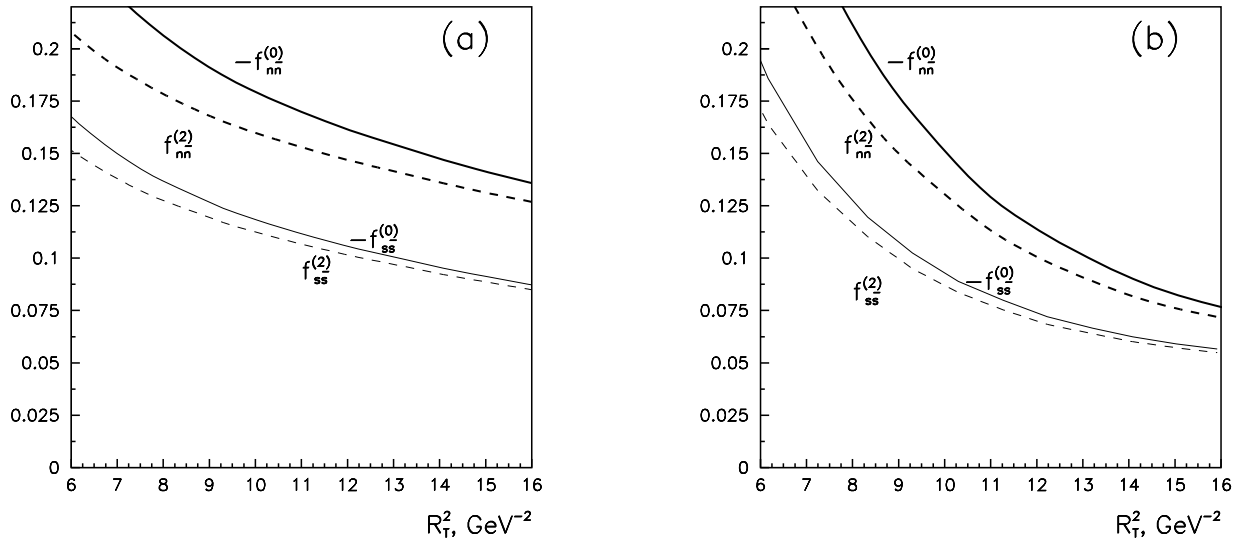


FIG. 10. Transition form factors in the decay of tensor quark-antiquark states  $1^3P_2 n\bar{n} \rightarrow \gamma\gamma$  and  $1^3P_2 s\bar{s} \rightarrow \gamma\gamma$  as functions of radius squared of the  $q\bar{q}$  system calculated with old (a) and new (b) photon wave functions.

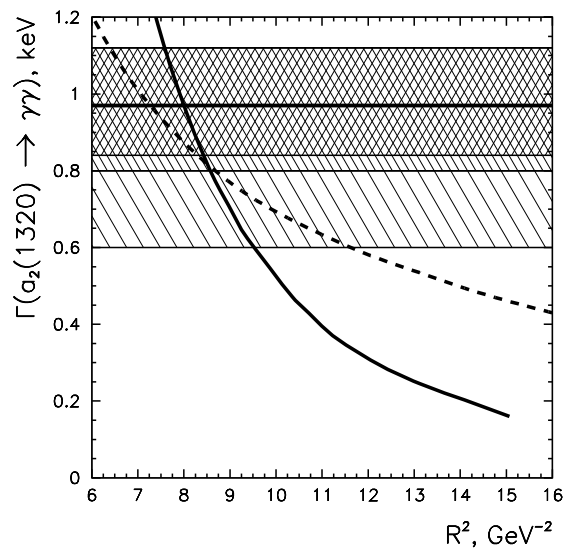


FIG. 11. Calculated curves *vs* experimental data (shaded areas) for  $\Gamma(a_2(1320) \rightarrow \gamma\gamma)$ . Solid curve stands for new photon wave function and dotted line for old one.

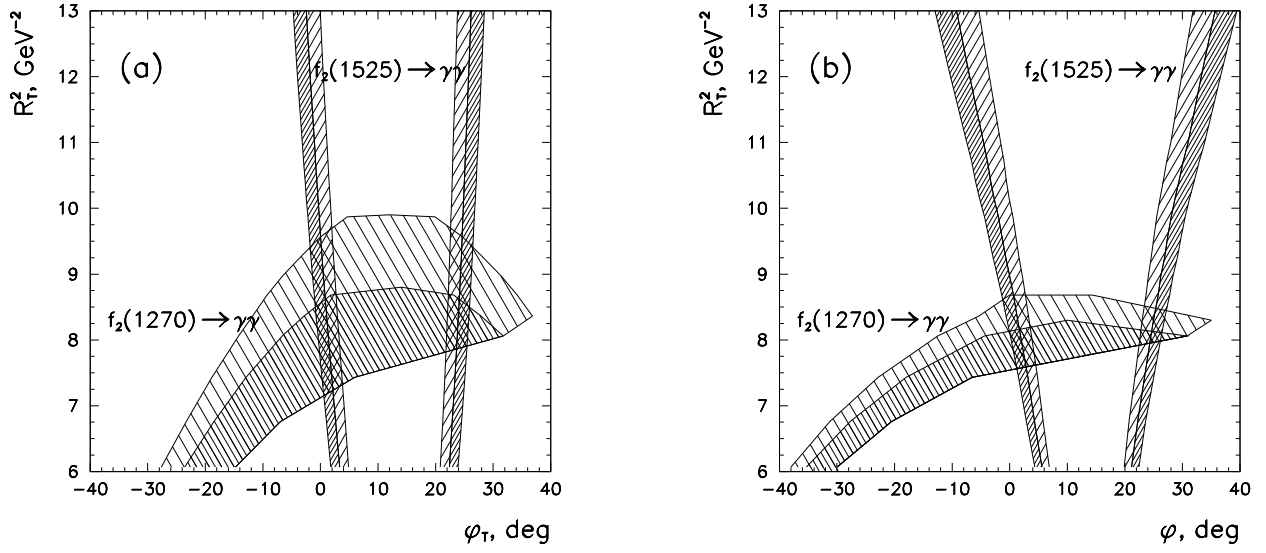


FIG. 12. Allowed areas  $(R_{f_0(980)}^2, \varphi)$  for partial widths  $\Gamma(f_2(1270) \rightarrow \gamma\gamma)$  and  $\Gamma(f_2(1525) \rightarrow \gamma\gamma)$  calculated with old (a) and new (b) photon wave functions. Mixing angle  $\varphi_T$  defines flavour content of mesons as follows:  $f_2(1270) = n\bar{n} \cos \varphi_T + s\bar{s} \sin \varphi_T$  and  $f_2(1525) = -n\bar{n} \sin \varphi_T + s\bar{s} \cos \varphi_T$ .